Improved Estimation of Neutrino Energy in Neutral Current Interactions with Liquid Argon Time Projection Chambers

Andrew P. Furmanski Christopher Hilgenberg

University of Minnesota

Motivation

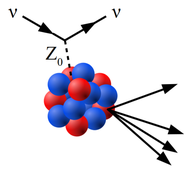

In NC scatters, the observables are the final state hadronic system kinematics. The total visible energy is a lower bound on the initial neutrino energy.

Liquid argon time projection chambers (LAr TPCs), with excellent tracking and calorimetry capabilities, are providing exquisite detail about neutrino interactions at few-GeV energies. This motivates new reconstruction methods.

Short-Baseline Neutrino Program (SBN)

Three, hundred-ton scale LAr TPCs are located along the Booster Neutrino Beam (BNB) at Fermilab. The BNB is broad-band, peaking at 600 MeV, with ν_e contamination ~0.5%.

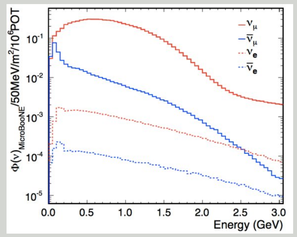

Figure 2. BNB flux at MicroBooNE

Table 1. SBN detector parameters used in this analysis. All values are taken from [2].

Detector	Active Mass [tons]	BNB Target Distance [m]	Exposure $\times 10^{20}$[POT]	Status
SBND	112	110	6.6	under construction
MicroBooNE	89	470	13.2	data taking complete
ICARUS	476	600	6.6	commissioning

Sterile neutrino search

SBN will probe the globally allowed, 3+1 sterile neutrino oscillation parameter space at high significance by simultaneously searching for ν_μ disappearance and ν_e appearance.

Toy Study

The BNB flux [2] was used to generate SBN-like samples. Each sample has 5×10^6 ν_μ and $\bar{\nu}_\mu$ interactions on Ar generated using GENIE v3.00.06 [3] with the G18_10a_02_11a tune.

We adopt the following simplifications and assumptions:

- ν production point is at the target
- No detector simulation or reconstruction
- Cheated reconstruction with Guassian smearing
- Neutrons with energies above 50 MeV can be tagged via inelastic scatters with 50% efficiency
- Neglect detector acceptance

Table 2. Assumed performances for LAr TPCs.

Species	Threshold [MeV]	Energy Res.	Angular Res. [deg]
p [4]	25	60 MeV	5
$\pi^\pm$ [5]	10	10%	2
γ [6]	30	10%	5

For this analysis, we consider several topologies relevant at BNB energies:

- NC inclusive → non-zero visible energy,
- NC0$\pi^\pm$ → reject if visible charged pion,
- NC1p + n-tag → 1 proton only.

The last two are far less susceptible to ν_μCC backgrounds. Charged pions and muons can be difficult to distinguish.

Neutrino Energy Estimation

Calorimetric reconstruction

Typically, the initial neutrino energy is estimated with a calorimetric measurement and a model dependent shape and scale correction.

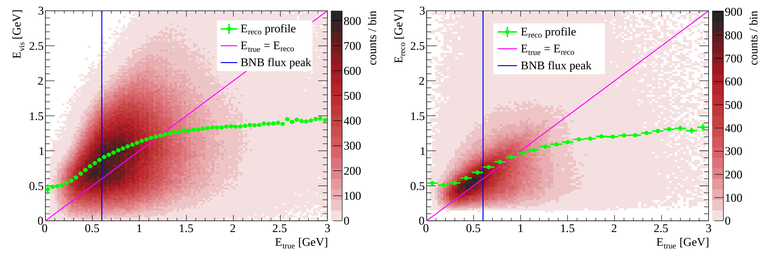

Figure 3. Reconstructed neutrino energy (vertical axis) vs. true energy (horizontal axis) for calorimetric (left) and kinematic (right) methods.

Kinematic reconstruction

The incident neutrino energy can be determined from the final state hadronic system kinematics if the neutrino scatters off a stationary, free nucleon with mass m_N.

The hadronic system is characterized by the total four-momentum, $(E_h, \vec{p_h})$. The angle relative to the beam axis is $\cos\theta_h = \vec{p_h} \cdot \hat{z}/|\vec{p_h}|$. The initial neutrino energy is then given by

$$E_\nu = \frac{p_h^2 - (E_h - m_N)^2}{2(m_N + p_h \cos\theta_h - E_h)}$$

If our assumption is violated, E_ν can be negative. In such cases, the event is rejected.

Reconstruction Performance

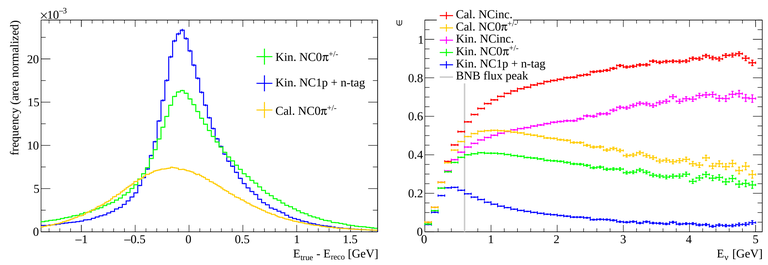

Figure 4. Neutrino energy resolution (left) and reconstruction efficiency (right) are shown for calorimetric and kinematic methods with different selections.

Comparing kinematic and calorimetric methods, using a NC0$\pi^\pm$ selection, the **kinematic method has better resolution with 75% lower bias and 45% lower FWHM**. but with **25% lower efficiency**.

Table 3. Reconstruction efficiencies integrated over all neutrino energies.

Method and Selection	Integrated Efficiency
Calorimetric NCinc	0.60
Calorimetric NC0$\pi^\pm$	0.47
Kinematic NCinc	0.45
Kinematic NC0$\pi^\pm$	0.37
Kinematic NC1p + n-tag	0.16

Less inclusive selections can improve resolution further. For the kinematic method, moving from NC0$\pi^\pm$ to NC1p + n-tag improves resolution by 30% but with a 60% lower efficiency.

Short-Baseline Sterile Neutrino Search via NC Disappearance

At short baselines, hypothetical eV-scale sterile neutrinos drive oscillations, described by the non-standard columns of the extended PMNS matrix. We focus on the 3+1 case: one sterile neutrino with mass-squared difference Δm^2_{41}.

NC disappearance is sterile neutrino appearance. For a pure ν_μ source, the appearance probability is given by

$$P_{\nu_\mu \to \nu_s} \simeq \sin^2(2\theta_{\mu s}) \sin^2\left(1.27 \Delta m^2_{41} \frac{L}{E_\nu}\right)$$

$\theta_{\mu s}$ is the effective mixing angle, L is the production-to-interaction distance, and E_ν is the neutrino energy.

3+1 Oscillation Sensitivity

Using a binned Poisson likelihood with the Asimov data set, we compare reconstructed neutrino energy spectra to evaluate the sensitivity.

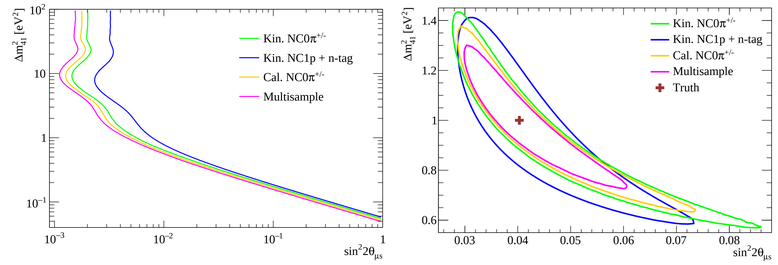

Figure 5. 1σ contours with statistical uncertainties only are shown without oscillations (left) and with $\sin^2 2\theta_{\mu s} = 0.04$, $\Delta m^2_{41} = 1\text{eV}^2$ (right).

The kinematic method is insufficient to compete with the calorimetric method in a statistics-limited measurement. However, we can adopt a .

A multi-sample approach is employed. Our sample splits into 3 sub-samples:

1. kinematic NC1p+n-tag
2. kinematic NC0$\pi^\pm$
3. calorimetric NC0$\pi^\pm$

If an event is rejected, it is passed to the next sub-sample. This maintains the same sample size while adding shape information. This approach yields the best sensitivities.

References

[1] Andrew P. Furmanski and Christopher Hilgenberg.
Neutrino energy estimation in neutral current interactions and prospects for sterile neutrino searches.
arXiv:2012.09788 [hep-ex], 2021.

[2] R. Acciarri, C. Adams, R. An, C. Andreopoulos, A.M. Ankowski, M. Antonello, *et al.* (MicroBooNE, LAr1-ND, and ICARUS-WA104 collaborations).
A proposal for a three detector short-baseline neutrino oscillation program in the Fermilab Booster Neutrino Beam.
arXiv:1503.01520 [hep-ex], 2015.

[3] C. Andreopoulos, A. Bell, D. Bhattacharya, F. Cavanna, J. Dobson, S. Dytman, et al.
The GENIE Neutrino Monte Carlo Generator.
Nucl. Instrum. Meth. A, 614:87–104, 2010.

[4] R. Acciarri, C. Adams, J. Asaadi, B. Baller, T. Bolton, C. Bromberg, et al.
Measurements of inclusive muon neutrino and antineutrino charged current differential cross sections on argon in the NuMI antineutrino beam.
Phys. Rev. D, 89:112003, Jun 2014.

[5] P. Abratenko, M. Alrashed, R. An, J. Anthony, J. Asaadi, A. Ashkenazi, et al.
First measurement of differential charged current quasielasticlike ν_μ-argon scattering cross sections with the MicroBooNE detector.
Phys. Rev. Lett., 125:201803, Nov 2020.

[6] C. Adams, M. Alrashed, R. An, J. Anthony, J. Asaadi, A. Ashkenazi, S. Balasubramanian, B. Baller, C. Barnes, G. Barr, et al.
Reconstruction and measurement of $\mathcal{O}(100)$ mev energy electromagnetic activity from $\pi^0 \to \gamma\gamma$ decays in the MicroBooNE LArTPC.
Journal of Instrumentation, 15(02):P02007–P02007, Feb 2020.